

# Current–voltage characteristic behaviour of dense $\text{Zn}_2\text{SnO}_4$ -ZnO ceramics

Y. Iglesias<sup>a,\*</sup>, M. Peiteado<sup>a</sup>, J. de Frutos<sup>b</sup>, A.C. Caballero<sup>a</sup>

<sup>a</sup> Departamento de Electrocerámica, Instituto de Cerámica y Vidrio, CSIC. C/Kelsen 5, Campus de Cantoblanco, 28049 Madrid, Spain

<sup>b</sup> Departamento de Física Aplicada, E.T.S.I. Telecomunicación, Universidad Politécnica de Madrid, Avda. de la Complutense s/n, 28040 Madrid, Spain

Available online 7 May 2007

## Abstract

The present work deals with the electrical characterization of undoped  $\text{Zn}_2\text{SnO}_4$  (ZTO) and  $\text{SnO}_2$ -doped ZnO bulk ceramics in order to clarify the role played by the ZTO spinel type phase in the electrical response of these materials. For this purpose,  $\text{SnO}_2$ -doped ZnO materials with  $\text{SnO}_2$  concentrations of 0.1, 1 and 10 mol% have been prepared by co-precipitation and undoped ZTO powders have been prepared by a classical mixing oxide procedure. ZTO materials with 90–92% of the theoretical density have been obtained and non-linear behaviour is observed for ZTO- and  $\text{SnO}_2$ -doped ZnO materials. For  $\text{SnO}_2$ -doped ZnO the appearance of non-linear  $I$ - $V$  behaviour is mainly dominated by the formation of the ZTO phase and the interfaces associated to its presence. ZTO shows a NTC behaviour that is in disagreement with the PTC behaviour previously reported in the literature.

© 2007 Published by Elsevier Ltd.

**Keywords:** ZnO;  $\text{Zn}_2\text{SnO}_4$ ; Electrical conductivity

## 1. Introduction

ZnO-based materials find a wide spectrum of applications both as bulk polycrystalline ceramics and films. The interest on these materials has been renewed because of their potential for obtaining transparent conductors, magnetic semiconductors and improved gas sensing elements.<sup>1</sup> For this purpose much research is being focused on the control of the ZnO electrical response by doping with different ions. Undoped ZnO crystallizes in the wurtzite structure and due to its native defects exhibits n-type conduction, however p-type conductivity can also be rendered by proper doping. Reported results on the role played by several dopants on the material microstructure and electrical response are often contradictory, actually basic issues as, for instance, the solid solubility limit of certain cations into the ZnO lattice are still unclear.<sup>2,3</sup> Data scattering in the literature is also favoured by the impact on the material reliability of the different processing used either for bulk materials or films.

Recently, the electrical behaviour of Sn-doped ZnO thin films grown by pulsed laser deposition (PLD) has been reported.<sup>4</sup> ZnO films with a nominal 0.1 mol%  $\text{SnO}_2$  show lower resistivity than undoped ZnO ones, this is in agreement with the incorporation of  $\text{Sn}^{4+}$  at  $\text{Zn}^{2+}$  lattice sites. However if  $\text{SnO}_2$

concentration is increased the electrical resistivity also increases and the cubic  $\text{Zn}_2\text{SnO}_4$  spinel type phase appears as a second phase. This secondary phase has also been observed in Sn-doped ZnO bulk ceramics but it appears even for the 0.1 mol%  $\text{SnO}_2$  concentration<sup>5</sup> which indicates that for polycrystalline materials, solid solubility limit of  $\text{SnO}_2$  into the ZnO lattice is below 0.1 mol%. The  $\text{Zn}_2\text{SnO}_4$  (ZTO) spinel phase has been synthesized as nanosized particles with different shapes<sup>6–9</sup> however few data have been found regarding the electrical behaviour of this pure phase. Reported data on ZTO thin films<sup>10</sup> show that their electrical resistivity is in the order of  $10^{-2} \Omega \text{ cm}$  as is also reported for ZnO films.<sup>1</sup> Therefore the formation of the ZTO phase itself cannot explain the electrical resistivity increase observed in Sn-doped ZnO films, however it seems plausible that the appearance of interfaces related to the formation of ZTO could play a significant role.

Current–voltage curves and electrical response of layered structures like  $\text{Zn}_2\text{SnO}_4/\text{ZnO}/\text{Pt}$  have been reported in the literature related to gas sensing applications.<sup>11,12</sup> ZTO samples with very fine grains show electrical resistivity values in the order of  $10^7 \Omega \text{ cm}$ ,<sup>11</sup> that is 9 orders of magnitude higher than reported for ZTO thin films. Nevertheless, these samples are very porous (40% of porosity in the sintered sample) and cannot be easily compared to the films or dense ceramic samples.

The present work deals with the electrical characterization of undoped  $\text{Zn}_2\text{SnO}_4$  and Sn-doped ZnO bulk ceramics in order to clarify the role played by the ZTO spinel type phase

\* Corresponding author.

E-mail address: [yiglesias@icv.csic.es](mailto:yiglesias@icv.csic.es) (Y. Iglesias).

in controlling the microstructure and therefore the electrical response of these materials.

## 2. Experimental procedure

SnO<sub>2</sub>-doped ZnO materials with SnO<sub>2</sub> concentrations of 0.1, 1 and 10 mol% were prepared by co-precipitation. Both Zn<sup>2+</sup> and Sn<sup>4+</sup> precursors (Zn(CH<sub>3</sub>COO)<sub>2</sub>·2H<sub>2</sub>O and SnCl<sub>4</sub>·5H<sub>2</sub>O) were dissolved in de-ionized water and mixed together to form a transparent solution. Concentrated NaOH (1 M) was added dropwise to the stirred solution to reach pH 10 and promote a complete precipitation of both cations. Precipitated powders were washed, filtered and treated at 450 °C. Zn<sub>2</sub>SnO<sub>4</sub> powders were prepared by a classical mixing oxide procedure. Stoichiometric amounts of high purity ZnO and SnO<sub>2</sub> were mixed and homogenized by ball milling in ethyl alcohol. Synthesis treatment was carried out at 1000 °C for 4 h. After this treatment only Zn<sub>2</sub>SnO<sub>4</sub> is detected by X-ray diffraction. Subsequent milling was performed to re-activate the particles and measured mean particle diameter gave a  $d_{50} = 2.8 \mu\text{m}$ .

Green pellets of 5 mm radius and 6 mm thickness were obtained by uniaxial pressing (120 MPa) and sintered in air between 1200 and 1300 °C for 2 h to reach apparent density values higher than 90% of the theoretical density. For subsequent characterization the outer surface of the samples was removed by grinding since evidence of Sn<sup>4+</sup> reduction was observed at this surface.

Crystalline phases present in the samples were characterized by X-ray diffraction (XRD) in a D-5000 Siemens Diffractometer using Cu K $\alpha$ 1 radiation. Microstructure analysis was carried out by Scanning Electron Microscopy (SEM) on both fracture and polished surfaces by using a field emission microscope Hitachi S-4700 and a Noran EDS detector.

For electrical characterization, sintered samples were lapped to 3 mm thick discs and Au electroded. Current–voltage measurements were done by using a DC power multimeter Keithley 2410.

## 3. Results and discussion

For the ZTO spinel phase, sintered pellets with 90–92% of the theoretical density were only obtained when sintered at 1250–1300 °C in a ZnO powder bed. After sintering, ZTO was the only phase detected by DRX. SEM micrograph of the fractured surface (Fig. 1) reveals different features. Very large grains are generally present in the sample, at localized regions between these large grains, much finer grains are observed forming small colonies. This gives a heterogeneous grain size distribution ranging around 3–70  $\mu\text{m}$ . Within the large ZTO grains appears closed residual porosity which is very difficult to remove and points out to the difficulty for sample densification. As it is known for SnO<sub>2</sub>, Sn<sup>4+</sup> reduction to Sn<sup>2+</sup> with the consequent oxygen loose may be the origin of this porosity. Microstructure characterization of the SnO<sub>2</sub>-doped ZnO materials studied in the present work reveals the characteristics mentioned above and recently discussed in the literature<sup>5</sup>: always two phases are observed and, increasing the SnO<sub>2</sub> obviously increases the ZTO amount but

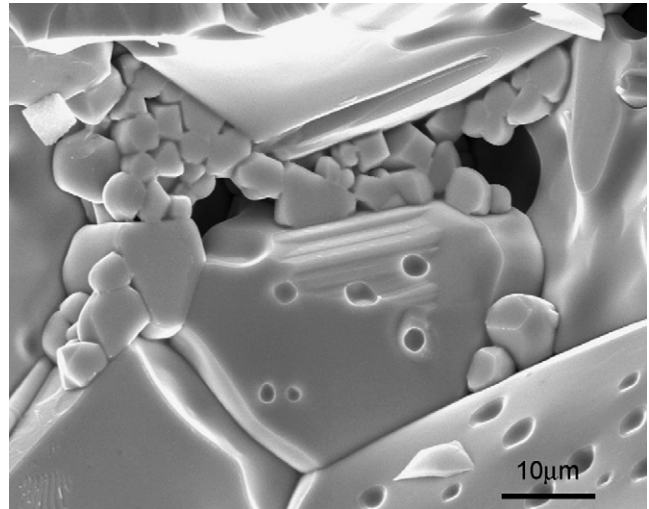


Fig. 1. SEM micrograph of fracture surface of a Zn<sub>2</sub>SnO<sub>4</sub> sample sintered at 1250 °C/2 h.

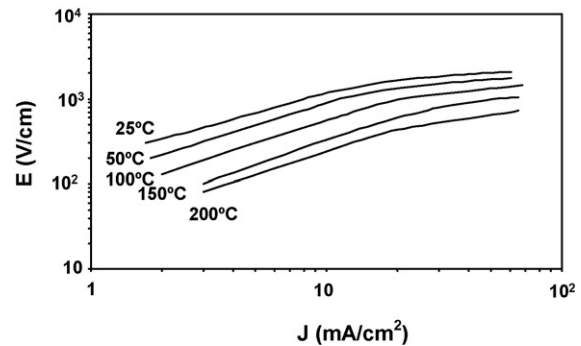


Fig. 2.  $I$ – $V$  curves for dense Zn<sub>2</sub>SnO<sub>4</sub> samples measured at different temperatures.

also ZnO grain size strongly decreases. According to reported data<sup>4,5</sup> solid solution limit must be even smaller than 0.1% SnO<sub>2</sub> and therefore ZnO grains might not be actually Sn-doped.

Fig. 2 shows the current–voltage behaviour observed for the ZTO materials at different temperatures.  $I$ – $V$  non-linear behaviour is observed for ZTO materials up to 200 °C. This non-linear behaviour is also common for all the SnO<sub>2</sub>-doped ZnO materials (Fig. 3). As it is well described for ZnO- and

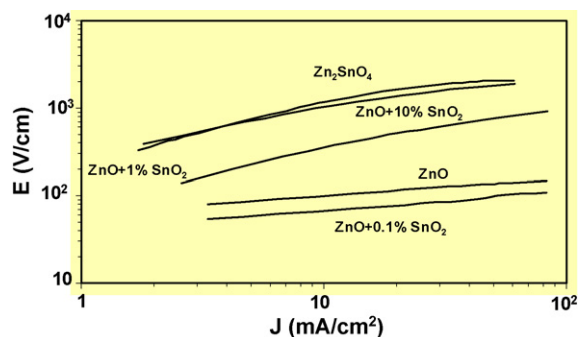


Fig. 3.  $I$ – $V$  curves measured at room temperature for Zn<sub>2</sub>SnO<sub>4</sub> and SnO<sub>2</sub>-doped ZnO dense samples.

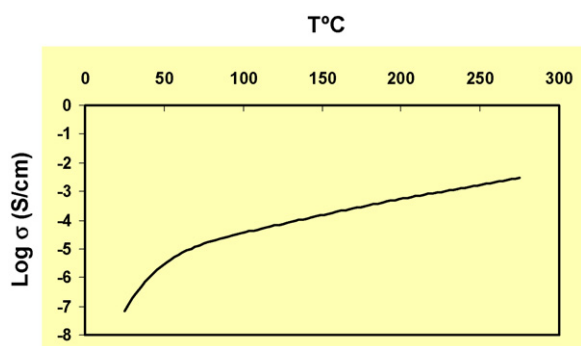


Fig. 4. DC conductivity against temperature for dense  $\text{Zn}_2\text{SnO}_4$ .

$\text{SnO}_2$ -based varistors, the formation of potential barriers at the grain boundaries is the origin of the  $I$ - $V$  non-linearity. Individual barrier characteristics depend on the specific nature of the grain boundary, i.e.,  $\text{ZnO}$ - $\text{ZTO}$  interphase or  $\text{ZnO}$ - $\text{ZnO}$  and  $\text{ZTO}$ - $\text{ZTO}$  homo-junctions. Moreover, since the macroscopic behaviour can be described as a series connection of the individual barriers,  $I$ - $V$  curve will be strongly dependant on both the  $\text{ZnO}/\text{ZTO}$  ratio and grain size since both features change the number and nature of grain boundaries. Comparing the  $I$ - $V$  curves of Fig. 3 obtained for the different materials it is clearly shown that the highest breakdown field and strongest non-linearity belongs to the ZTO sample. From the microstructure point of view, ZTO material grain size is very heterogeneous and the largest when compared to the  $\text{SnO}_2$ -doped  $\text{ZnO}$  and undoped  $\text{ZnO}$  samples. Both features work against the ZTO  $I$ - $V$  curve since large and heterogeneous grain sizes decreases the number of interfaces and lead to current localization decreasing the field and non-linearity of the curve. Therefore, ZTO non-linearity must be originated directly on a higher intrinsic potential barrier height at the  $\text{ZTO}/\text{ZTO}$  grain boundaries. For  $\text{SnO}_2$ -doped  $\text{ZnO}$  the appearance of non-linear  $I$ - $V$  behaviour is mainly dominated by the formation of the ZTO phase and the interfaces associated to its presence.

Fig. 4 shows the DC conductivity against temperature for a dense ZTO sample. The curve reflects a continuous increase of the conductivity with temperature. This result is in disagreement with Yu and Choi.<sup>11</sup> These authors reported the existence of PTC behaviour for porous ZTO samples below 150 °C, however our results on dense ZTO do not show this effect. The reasons for such discrepancies might be related to two different points. First, the authors did not take into account the non-linearity of the current-voltage curve for such temperatures and second, it has been shown that in porous materials with this level of conductivity relative humidity can control the electrical response.<sup>13</sup> If this second hypothesis is true, then the increase of the resistivity attributed to PTC behaviour is only related to a “drying” effect at temperatures above 100 °C.

#### 4. Conclusions

ZTO materials with 90–92% of the theoretical density have been obtained sintering at 1250–1300 °C in a  $\text{ZnO}$  powder bed. Microstructure shows a heterogeneous grain size distribution ranging around 3–70  $\mu\text{m}$ .  $I$ - $V$  non-linear behaviour is observed for ZTO materials up to 200 °C. This non-linear behaviour is also common for the  $\text{Sn}$ -doped  $\text{ZnO}$  materials. ZTO non-linearity is originated directly on a higher intrinsic potential barrier height at the  $\text{ZTO}/\text{ZTO}$  grain boundaries. For  $\text{SnO}_2$ -doped  $\text{ZnO}$  the appearance of non-linear  $I$ - $V$  behaviour is mainly dominated by the formation of the ZTO phase and the interfaces associated to its presence. ZTO shows a NTC behaviour that is in disagreement with the PTC behaviour previously reported in the literature.

#### References

1. Pearton, S. J., Norton, D. P., Ip, K., Heo, Y. W. and Steiner, T., Recent progress in processing and properties of  $\text{ZnO}$ . *Prog. Mater. Sci.*, 2005, **50**, 293–340.
2. Costa-Kramer, J. L., Briones, F., Fernández, J. F., Caballero, A. C., Villegas, M., Díaz, M. *et al.*, Nanostructure and magnetic properties of the  $\text{MnZnO}$  system, a room temperature magnetic semiconductor? *Nanotechnology*, 2005, **16**(2), 214–218.
3. Peiteado, M., Iglesias, Y., de Frutos, J., Fernández, J. F. and Caballero, A. C., Preparation of  $\text{ZnO}$ - $\text{SnO}_2$  ceramic materials by a co-precipitation method. *Bol. Soc. Esp. Ceram. V*, 2006, **45**(3), 158–162.
4. López-Ponce, E., Costa-Krämer, J. L., Martín-González, M. S., Briones, F., Fernández, J. F., Caballero, A. C. *et al.*, Growth and characterization of  $\text{Sn}$  doped  $\text{ZnO}$  thin films by pulsed laser deposition. *Phys. Stat. Sol. (a)*, 2006, **203**(6), 1383–1389.
5. Peiteado, M., Iglesias, Y., Fernández, J. F., de Frutos, J. and Caballero, A. C., Microstructural development of tin doped  $\text{ZnO}$  bulk ceramics. *Mater. Chem. Phys.*, 2007, **101**, 1–6.
6. Fang, J., Huang, A., Zhu, P., Xu, N., Xie, J., Chi, J. *et al.*, Hydrothermal preparation and characterization of  $\text{Zn}_2\text{SnO}_4$  particles. *Mater. Res. Bull.*, 2001, **36**, 1391–1397.
7. Wang, C., Wang, X., Zhao, J., Mai, B., Sheng, G., Peng, P. *et al.*, Synthesis, characterization and photocatalytic property of nano-sized  $\text{Zn}_2\text{SnO}_4$ . *J. Mater. Sci.*, 2002, **37**, 2989–2996.
8. Wang, J. X., Xie, S. S., Yuan, H. J., Yan, X. Q., Liu, D. F., Gao, Y. *et al.*, Synthesis, structure, and photoluminescence of  $\text{Zn}_2\text{SnO}_4$  single-crystal nanobelts and nanorings. *Solid State Commun.*, 2004, **131**, 435–440.
9. Wang, J. X., Xie, S. S., Gao, Y., Yan, X. Q., Liu, D. F., Yuan, H. J. *et al.*, Growth and characterization of axially periodic  $\text{Zn}_2\text{SnO}_4$  (ZTO) nanostructures. *J. Cryst. Growth*, 2004, **267**, 177–183.
10. Young, D. L., Moutinho, H., Yan, Y. and Coutts, T. J., Growth and characterization of radio frequency magnetron sputter-deposited zinc stannate,  $\text{Zn}_2\text{SnO}_4$ , thin films. *J. Appl. Phys.*, 2002, **92**(1), 310–319.
11. Yu, J. H. and Choi, G. M., Current-voltage characteristics and selective CO detection of  $\text{Zn}_2\text{SnO}_4$  and  $\text{ZnO}/\text{Zn}_2\text{SnO}_4$   $\text{SnO}_2/\text{Zn}_2\text{SnO}_4$  layered-type sensors. *Sens. Actuators B Chem.*, 2001, **72**, 141–148.
12. Wagh, M. S., Patil, L. A., Seth, T. and Amalnerkar, D. P., Surface cupricated  $\text{SnO}_2$ - $\text{ZnO}$  thick films as  $\text{H}_2\text{S}$  gas sensors. *Mater. Chem. Phys.*, 2004, **84**, 228–233.
13. Caballero, A. C., Villegas, M., Fernández, J. F., Viviani, M., Buscaglia, M. T. and Leoni, M., Effect of humidity on the electrical response of porous  $\text{BaTiO}_3$  ceramics. *J. Mater. Sci. Lett.*, 1999, **18**, 1297–1299.